American Mineralogist, Volume 69, pages 1082–1089, 1984

Alternative interpretation of diffraction patterns attributed to low ($P2_1ca$) orthopyroxene

SATOSHI SASAKI,[1] CHARLES T. PREWITT

Department of Earth and Space Sciences
State University of New York
Stony Brook, New York 11794

AND GEORGE E. HARLOW
Department of Mineral Sciences
American Museum of Natural History
New York, New York 10024

Abstract

Although there are several reports of $P2_1ca$ orthopyroxene, detailed investigations of the limited published data and of unpublished pyroxene diffraction patterns have revealed that almost all reported "forbidden reflections" violating the systematic absences $k = 2n$ on ($0kl$) of *Pbca* orthopyroxene can be explained as (I) reflections from *C2/c* clinopyroxene exsolved on (100) with fortuitously-similar cell dimensions that yield congruent diffraction with supposed $P2_1ca$ orthopyroxene, (II) diffuse streaks of either orthopyroxene and/or clinopyroxene from the neighboring levels of the ($0kl$) plane, and (III) multiple diffraction effects. The "forbidden reflections" 032, 052, 072, 011 2, 016, 056, 076, and 0 11 6 are caused by (I); those of 011, 031, 051, 071, 091, 033, 053, 073, 093, 014, 034, 054, 074, 015, and 035 result from (II); those of 011, 012, and 034 can be the result of (III). Only a few faint reflections do not appear to be adequately explained by (I)–(III), but these are not sufficient evidence for the existence of $P2_1ca$ orthopyroxene.

Introduction

Orthopyroxene, $(Mg,Fe)SiO_3$, is a common mineral of considerable geological importance because of its widespread occurrence in igneous and metamorphic rocks and because of its use as an indicator of geologic processes and history. This mineral is orthorhombic (*Pbca*), having the cell dimensions: a = 18.2–18.4Å, b = 8.8–9.1Å, and c = 5.2–5.3Å. In routine examinations of orthopyroxene, modifications with the space group $P2_1ca$ have been reported from lunar rocks (Smyth, 1974; Smyth, 1975; Steele, 1975; Nord et al., 1976) and meteorites (Harlow et al., 1979; Evensen et al., 1979; Harlow, 1980). In examinations of the relationship between real pyroxene and amphibole structures and theoretical topological models based on closest packing of oxygen, Thompson (1970) and Papike et al. (1973) noted that the model orthopyroxene should have symmetry lower than *Pbca*, and indeed, the $P2_1ca$ symmetry. Consequently, more significance was attributed to recognition of this pyroxene space group modification than would have been otherwise. Smyth (1974) and Harlow et al. (1979) suggested that the $P2_1ca$ modification was a lower (more ordered than *Pbca* pyroxene) structural state (hence the term low orthopyroxene) caused by very slow cooling or long annealing, and additional evidence was found for low orthopyroxene in slowly-cooled rocks (Harlow, 1980). In these studies, identification of low orthopyroxene was based on the presence of reflections that violate the systematic absences for a *b*-glide plane in *Pbca*. However, such identification is not wholly satisfactory because: (1) The crystals reported to date are not single crystals, but always include exsolved phases, usually augite; (2) in many cases either orthopyroxene and/or exsolved augite have diffuse streaks parallel to the common **a*** axes; and (3) because of the frequent occurrence of Umweganregung reflections, care must be taken to evaluate the possibility that this effect produced the reflections in question (Sasaki and Matsumoto, 1977; Sasaki et al., 1981). Therefore, a detailed examination of the limited published data and of numerous unpublished diffraction patterns of orthopyroxene and clinopyroxene was carried out to evaluate the "forbidden reflections." The results of the investigation are presented in this paper.

Results

There are at least three possible sources for reflections that violate the systematic absences for *Pbca* orthopyrox-

[1] Present address: National Laboratory for High Energy Physics, Oho-machi, Tsukuba-gun, Ibaraki-ken, 305, Japan.

0003–004X/84/1112–1082$02.00

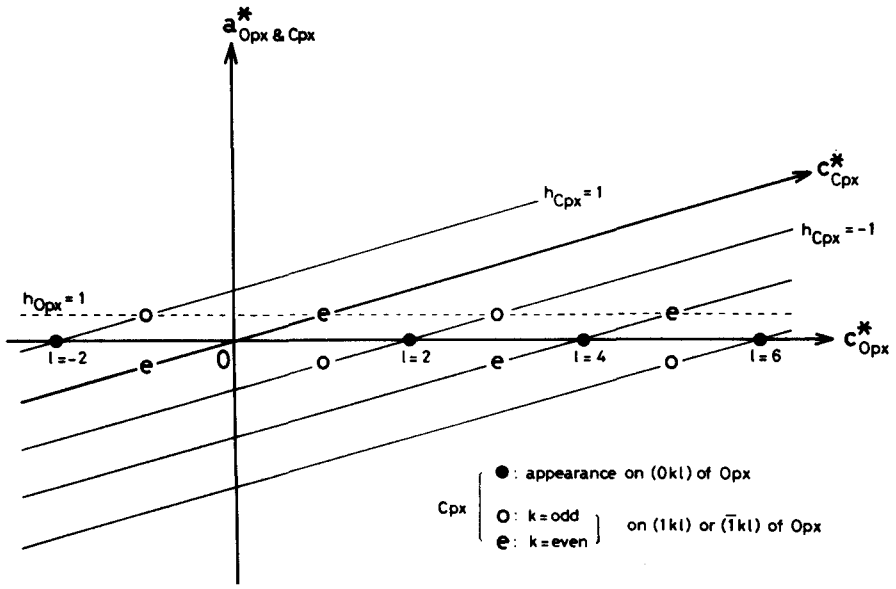

Fig. 1. A projection down **b*** of reciprocal lattice layers for Opx and (100)-exsolved *C*2/*c* Cpx.

ene and yield an apparent $P2_1ca$ space group: Reflections from a second exsolved phase with a particular orientation and fortuitously-similar cell parameters (Type I reflections); diffuse streaks from adjacent upper-levels of both orthopyroxene and *C*2/*c* (and possibly $P2_1/c$) clinopyroxene (Type II reflections); and multiple diffraction effects (Type III reflections).

Type I: Coexisting C2/c clinopyroxene

Because most reports refer to the existence of augite exsolved on (100) of orthopyroxene (Opx), we first consider the case of *C*2/*c* clinopyroxene (Cpx) in the Opx matrix, where Opx and Cpx have common **a*** and **b*** axes (Fig. 1). It must be emphasized that the "normal" separa-

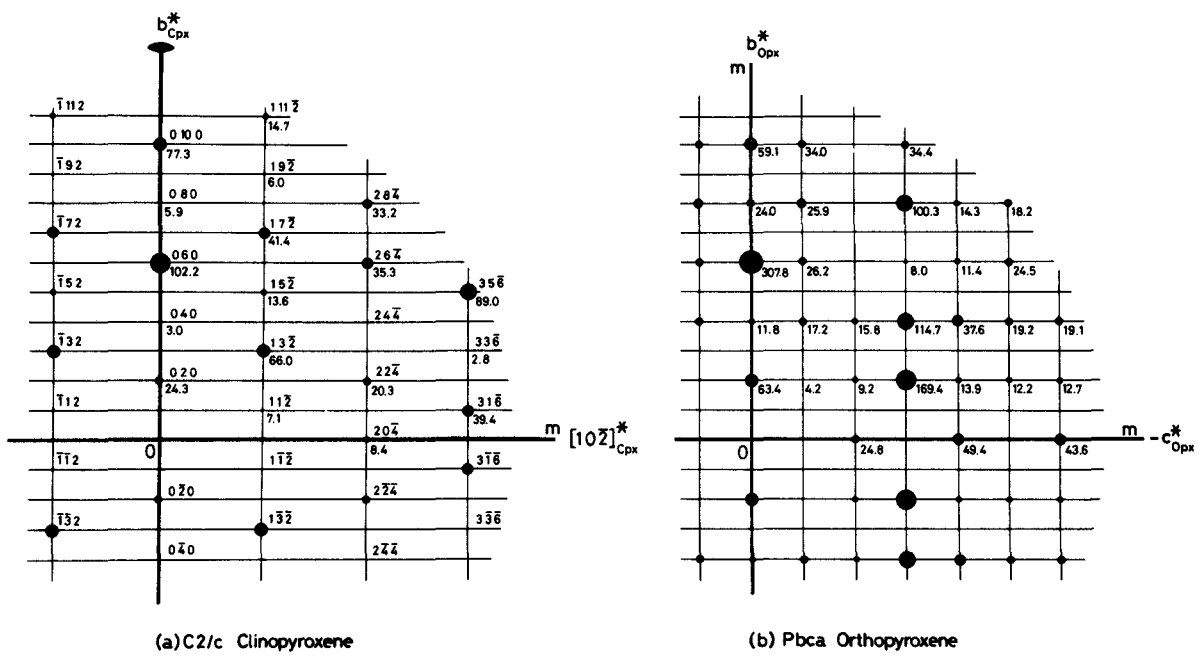

Fig. 2. Schematic distribution of structure factors on $(0kl)_{Opx}$ from (a) exsolved *C*2/*c* Cpx and (b) Opx. The numerals to the lower and upper right sides of each spot are the values of the structure factor and Miller indices, respectively. The sizes of the circles are approximately proportional to the magnitudes of the structure factors.

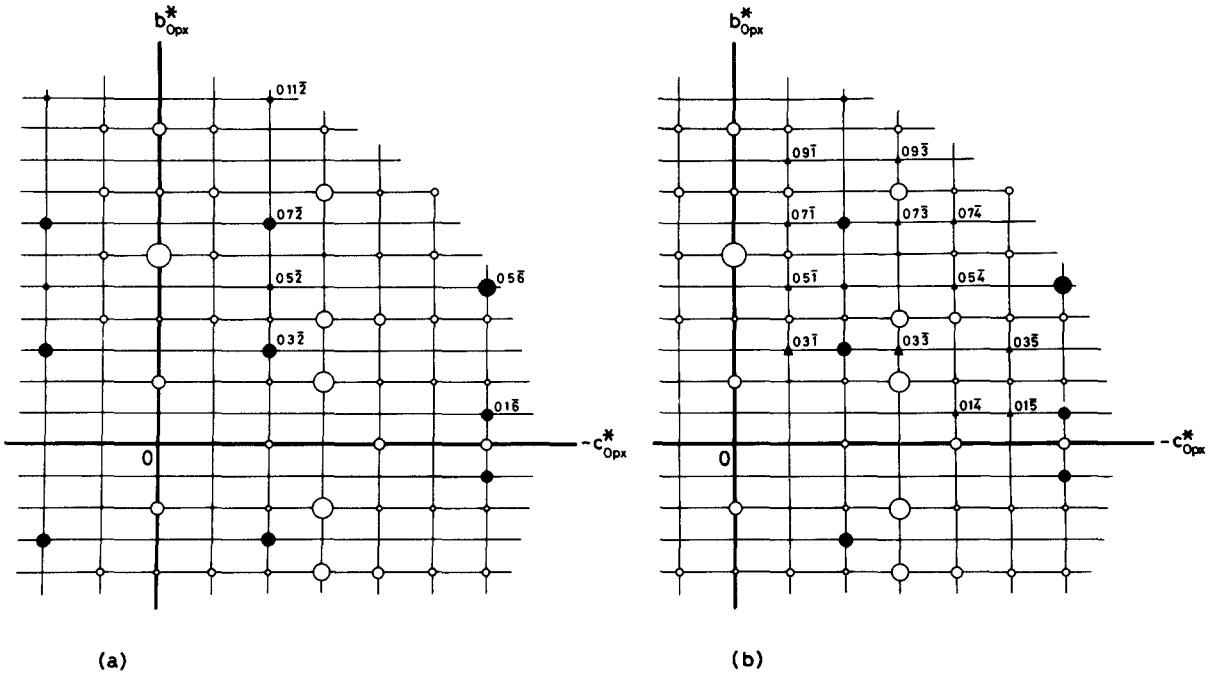

Fig. 3. Final distribution of structure factors on $(0kl)_{Opx}$ (a) including only reflections of exsolved $C2/c$ Cpx and (b) including both reflections of exsolved Cpx and diffuse streaks from Opx and Cpx. The triangles in (b) indicate an estimate of the proportional intensity of diffuse streaks intersecting $(0kl)_{Opx}$. The sizes of the circles are approximately proportional to the magnitudes of the structure factors.

tion of diffraction spots may not occur in some Opx–Cpx intergrowths; cell parameters may be so related that it is impossible to distinguish, by position on a photograph, the separate reflections of the two-phase intergrowth. As can be seen in Figure 1, the diffraction spots of Cpx with indices l = *even* in register appear on the $(0kl)_{Opx}$ net, when $[\bar{1}02]^*_{Cpx} = \mathbf{c}^*_{Opx}$. All such $C2/c$ Cpx spots occur under the following conditions: when $k_{Cpx,Opx}$ = *odd*, h_{Cpx} must also be odd and when $k_{Cpx,Opx}$ = *even*, h_{Cpx} must be even (by reason of C-centering absences). The reflections with k_{Cpx} = *even* superimpose on the Opx reflections in the $(0kl)_{Opx}$ net. The Cpx reflections with $l = \pm 2, \pm 6$, and so on are in register with k = *odd* nodes of the $(0kl)_{Opx}$ net, and thus apparently violate the b-glide plane condition. In the case of $P2_1/c$ Cpx, spots are possible for all $0kl_{Opx}$ where l = *even*. Figure 2a shows schematic distributions of the structure factors of a $C2/c$ Cpx contributing to $(0kl)_{Opx}$, compared with those of Opx in Figure 2b. It should be noted that the intensity distribution of Cpx reflections on the $\mathbf{b}^*$-$[10\bar{2}]^*$ plane have *mm* symmetry, the same as for $(0kl)_{Opx}$. In Figure 2, the Miller index and the crystal structure factor, $|F_{obs}(hkl)|$, are shown to the upper right and lower right of each diffraction spot, respectively. The structure factors, rather than intensities, of diopside for Cpx and orthoenstatite for Opx (Sasaki et al., 1980) are used here to indicate the strength of diffraction spots. A diffraction pattern based on reflections from both Opx and Cpx is shown in Figure 3a, where the volume ratio Opx:Cpx is assumed to be 1:1 (not as large as is likely in real crystals). The above construction shows that the extra reflections 032, 052, 072, 0 11 2, 016, 056, 076, and 0 11 6 have measureable contributions from the exsolved Cpx. If $P2_1/c$ Cpx contributes significantly to the diffraction pattern, the reflections 012, 014, and 074 may be present (based on the structure factor tables for a lunar pigeonite from Ohashi and Finger, 1974). Thus, by themselves, the above reflections are not proof of the existence of $P2_1ca$ orthopyroxene.

Type II: Diffuse streaks from upper levels

Orthopyroxenes with very fine (100) exsolution and/or Guinier–Preston zones are known to exhibit diffuse streaking along $\mathbf{a}^*$ in diffraction photographs (cf. Miyamoto et al., 1975; Nord, 1980). The effect is common in lunar and meteoritic pyroxenes; diffraction patterns of these pyroxenes also often show diffuse streaks caused by shock effects (Reid et al., 1974; Takeda, personal communication). Because the $\mathbf{a}^*$ dimension is short on diffraction photographs (2.3 mm for a 60 mm focal length precession camera using Mo$K\alpha$ X-rays for a typical bronzite), diffuse streaks can and do overlap with neighboring $\mathbf{a}$-axis levels. In the case of very fine (100) lamellae of Cpx, there is the possibility of diffuse streaking onto $(0kl)_{Opx}$ from two sources: one from $\pm 1kl_{Opx}$ and the other from adjacent Cpx levels. Figure 1 shows schematically

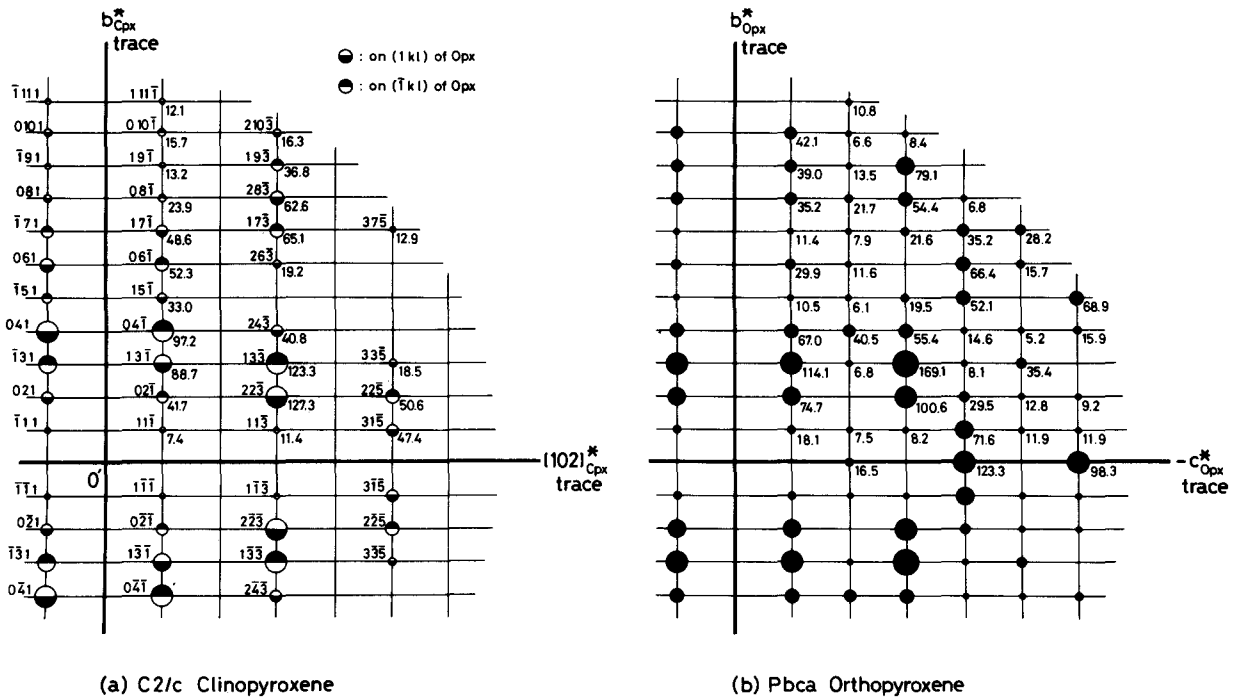

Fig. 4. Schematic diffraction patterns on reciprocal lattice levels that are shifted 1/18.3 (A^{-1}) along the **a*** axis parallel to $(0kl)_{Opx}$. (a) *C2/c* Cpx exsolution on (100); and (b) $(1kl)_{Opx}$ of Opx. The numerals represent the values of the structure factors and Miller indices as in Fig. 2. The sizes of the circles are approximately proportional to the magnitudes of the structure factors.

the relationship between the upper Cpx levels and the **a*c*** 0-level for Opx. It should be emphasized that the Cpx has essentially the same short spacing along the **a*** axis as does Opx for the planes adjacent to $(0kl)_{Opx}$. Consequently, diffuse streaks along the **a*** axis from Cpx could produce spots corresponding to $(0kl)_{Opx}$. The diffuse streaks of Cpx can only intersect $(0kl)_{Opx}$ if l is odd; that is when Cpx reflections correspond to $(\pm 1kl)$ of Opx (see Fig. 1). The indices for these relevant Cpx reflections are also constrained to have $h + k = 2n$ due to *C* centering in *C2/c* Cpx lamellae. Thus, there is only one reflection, equivalent either to $1kl_{Opx}$ or $\bar{1}kl_{Opx}$ for each value of kl (see Figs. 1 and 4a). For example, when $l = 1$, the reflections with $k_{Cpx} = even$ appear on $(1kl)_{Opx}$, whereas those with $k_{Cpx} = odd$ appear on $(\bar{1}kl)_{Opx}$. The case for $P2_1/c$ pyroxene lamellae is more general, with the same restriction applying to l odd; however, both $1kl_{Opx}$ and $\bar{1}kl_{Opx}$ reflections (not equivalent) are present for each set of kl's, and the odd/even restrictions in Figures 1 and 4a do not apply. Only *C2/c* Cpx is modelled in the figures that follow, although potential contributions from $P2_1/c$ Cpx were calculated as shown below. The distributions of structure factors for appropriate upper levels of Cpx and Opx are shown to the lower right of each diffraction spot in Figures 4a and 4b, respectively. The reciprocal lattice level shown in Figure 4 is shifted 1/18.3 (A^{-1}) along the $\mathbf{a}^*_{Opx,Cpx}$ axes from $(0kl)_{Opx}$ (the effective $\mathbf{a}^*_{Cpx}$ repeat is slightly less $\simeq 1/18.7 \simeq 1/a \sin\beta$). The Miller indices of Cpx are indicated at the upper left side of each reflection in Figure 4a. The distribution of diffuse streaks of both Opx and Cpx results in *mm* symmetry, consistent with the $(0kl)_{Opx}$ plane.

By combining Figures 4a and 4b, the intensity distribution of diffuse streaks was estimated on $(0kl)_{Opx}$ and is shown with triangle symbols in Figure 3b. The structure factors of upper-level reflections are summarized in Table 2; only structure factors that may have a contribution above those of type I are listed. The "forbidden reflections" 031, 033, 093, and 035 can be caused by streaks from reflections of both Opx and Cpx; the "forbidden reflections" 051, 071, 073, and 015 on $(0kl)_{Opx}$ can be due to upper-level streaks of Cpx, and those of 091, 014, 034, 054, and 074 can be from streaks of Opx. Of these, 031 and 033 have especially strong intensities. Again, if $P2_1/c$ Cpx occurs in significant abundances as very fine lamellae, upper-level streaks may contribute to reflections 011, 031, 051, 091, 013, 033, 053, 093, 035, and 017. The "forbidden reflections" 011, 092, and 053 may be also explained as streaks of Opx, although the intensities are only intermediate (see Table 2). Reflections 012, 055, and 036 have very little contribution from either Type I or II diffraction mechanisms. X-ray photographs on $(h1l)$, $(h3l)$, and $(hk1)$ should resolve this question, as will be shown subsequently. Moreover, the relative intensity of those "forbidden reflections" caused by upper-level Cpx versus Opx reflection streaking should vary as the rela-

Table 1. Summary of reflections reported in support of $P2_1ca$ orthopyroxene. The reports of Huebner et al. (1975) are excluded because no indices were given and the reports of Evensen et al. (1979) and Harlow (1980) are superceded by the data given here for Johnstown bronzite and enstatite from Zimbabwe.

	Smyth (1974)		Smyth (1975)	Steele (1975)	Nord et al.* (1976)		Serra de Magé**	Johnstown Bronzite	Zimbabwe Enstatite
	P	D							
Type I: Resulting from exsolved C2/c Cpx									
0 1 2							E	o	o
0 3 2	E	E		o			o	o	o
0 5 2		o					o	o	o
0 7 2	E	E	o	o			o	o	o
0 11 2		o					o		
0 1 6	E		o			E	o	o	o
0 5 6	E	E	o			E	o	o	o
0 7 6		o					o	o	o
0 11 6		o							
Type II: Resulting from upper-level diffuse streaks of Opx and/or Cpx									
0 1 1	o		o					o	E
0 3 1	E			o		E		o	E
0 5 1	o	o	o					o	o
0 7 1	o	o	o	o				o	o
0 9 1	o	o	o					o	o
0 3 3	E					E	E	E	E
0 5 3	o	o	o					o	o
0 7 3								o	o
0 9 3		o						o	o
0 1 4	o	o	o	o				o	o
0 7 4								o	o
0 1 5	o		o	o				o	o
0 3 5	o	o						o	o
0 3 7								o	o
Type III: Resulting from multiple diffraction									
0 1 1	o		o						
0 1 2		o							
0 3 4		o							

o Reported as evidence to support $P2_1ca$ orthopyroxene.
E Observed but eliminated from consideration by the respective authors.
P Precession camera data.
D Four-circle diffractometer data.
* There are forbidden reflections of other types, although the indices are not shown in their paper.
** Reported in Harlow et al. (1979), but also observed in this study.

tive proportion of Cpx and Opx in an exsolved crystal (see Table 2); this relationship should be another test for the validity of the interpretation.

Type III: Multiple diffraction

The influence of multiple diffraction in Opx and Cpx was described elsewhere (Sasaki et al., 1981). Therefore, we only need to state that a check for this effect should be made after eliminating reflections of additional phases. Although, in the precession method, the specific condition for multiple diffraction can usually be avoided by changing the θ angle or crystal orientation (Burbank, 1965), it should be noted that the avoidable condition depends on factors such as the weakness of detectable intensity, the wavelength used, and the degree of filling of the reciprocal lattice.

Discussion

For much of the published literature, it is difficult to evaluate the thoroughness of the search for diffraction from exsolved phases or for multiple diffraction. In this section, we first review published data and then our own data with respect to the criteria for unquestionable "forbidden reflections."

Table 1 contains a summary of previously-reported reflections as well as new data that were used to support the existence of $P2_1ca$ orthopyroxene. Unfortunately, none of the reports except for Smyth's (1974) original study were accompanied by X-ray diffraction photographs, and most reports do not state the Miller indices of the "forbidden reflections." However, we have reexamined photographs used in some previous studies (Harlow et al., 1979; Harlow, 1980) and include a summary of these data here. Table 1 is organized by the possible type of source that can produce the apparent "forbidden reflections." It is obvious from Table 1 that there are inconsistencies among the different sets of data reported and that all data cannot represent low orthopyroxene or any single phase.

The two best documented examples are inverted pigeonite from the Serra de Magé meteorite (Harlow et al., 1979; Harlow, 1980) and lunar 76535 bronzite (Smyth, 1974; 1975). The former represents the simple case of Type I Cpx diffraction. All extra spots are consistent with Type I Cpx reflections; no other types occur, and no diffuseness or streaking of reflections was found. The 76535 pyroxene can be explained as a combination of all

Table 2. The structure factors, ideal intensities, and scattering angles for upper-level reflections of Opx and Cpx. Indices are given relative to the Opx axes. Only those reflections are listed that have intensities greater than those of Cpx on $(0kl)_{Opx}$.

		Opx	Cpx	$P2_1/c$ Cpx	Upper-level reflections		
$(0kl)_{Opx}$	$2\theta_{Mo}$	$\lvert F_{obs}\rvert$	$\lvert F_{obs}\rvert$	$\lvert F_{obs}\rvert$	I'	I''	I'''
0 1 1	9.1	18.1	7.4	26.7:16.0	237	303	349
0 3 1	16.0	114.1	88.7	90.3:26.1	11300	12550	11414
0 5 1	24.6	10.5	33.0	23.3:27.0	437	199	197
0 7 1	33.7	11.4	48.6	9.4: 6.6	874	333	119
0 9 1	43.3	39.0	13.2	35.1: 3.4	1070	1399	1329
0 1 2	16.4	7.5	-	-	38	51	47
0 9 2	45.6	13.5	-	-	122	166	152
0 1 3	24.1	8.2	11.4	33.3: 5.5	88	73	119
0 3 3	27.6	169.1	123.3	102.2:76.1	24100	27377	25154
0 5 3	33.5	19.5	-	30.9:10.4	254	346	388
0 7 3	40.9	21.6	65.1	5.4:12.4	1730	809	402
0 9 3	49.3	79.1	36.8	42.9:39.5	4620	5898	5497
0 1 4	32.2	71.6	-	-	3420	4661	4272
0 3 4	34.9	29.5	-	-	580	791	725
0 5 4	39.8	52.1	-	-	1810	2468	2262
0 7 4	46.4	35.2	-	-	826	1126	1033
0 1 5	40.4	11.9	47.4	12.2: 1.6	843	333	126
0 3 5	42.7	35.4	18.5	6.1:56.3	950	1170	1207
0 5 5	47.0	-	-	4.8: 8.4	-	-	7
0 7 5	52.7	28.2	12.9	11.3:18.0	586	738	698
0 3 6	50.9	-	-	-	-	-	-
0 5 6	54.6	68.9	-	-	3160	4316	3956
0 1 7	57.8	25.5	28.8	6.1:23.4	710	667	578
0 3 7	59.5	13.9	25.3	6.3: 3.7	342	234	165

\- No intensity or weak

$I' = (2|F|^2_{Opx} + |F|^2_{Cpx})/3$ -- Opx:Cpx = 1:1

$I'' = (10|F|^2_{Opx} + |F|^2_{Cpx})/11$ -- Opx:Cpx = 5:1

$I''' = (10|F|^2_{Opx} + |F(h)|^2_{Cpx} + |F(\bar{h})_{Cpx})/12$ -- Opx:Cpx($P2_1/c$) = 5:1

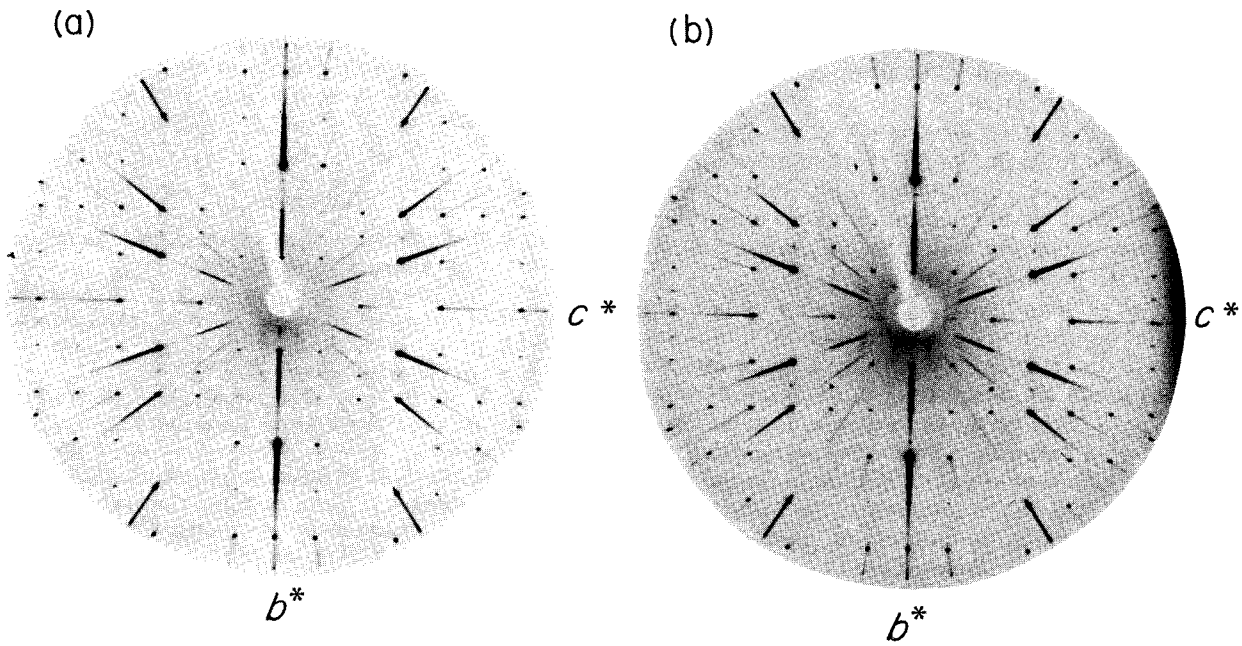

Fig. 5. Long-exposure precession photographs (Mo$K\alpha$;$\bar{\mu}$ = 27°; 100 hours) of (0kl) for (a) Johnstown bronzite (AMNH 2495) and (b) enstatite from Zimbabwe (BMNH 1933, 407) Both contain fine exsolution of Cpx on (100) that yields Cpx reflections lying exactly on Opx lattice points. Note strong 032, 016, 056, and fuzzy 033 reflections, discussed in the text.

three types of reflections. Smyth (1974) eliminated all Type I reflections from his photographic data, but reported diffractometer data (also Smyth, 1975) that are still consistent with these Cpx reflections. After the reflections of Types I and II are excluded, the reflections 012, 034, 011, and 053 remain. According to Smyth (1974), the 011 reflection only appeared on precession photographs, whereas those of 012 and 034 were only detected on the

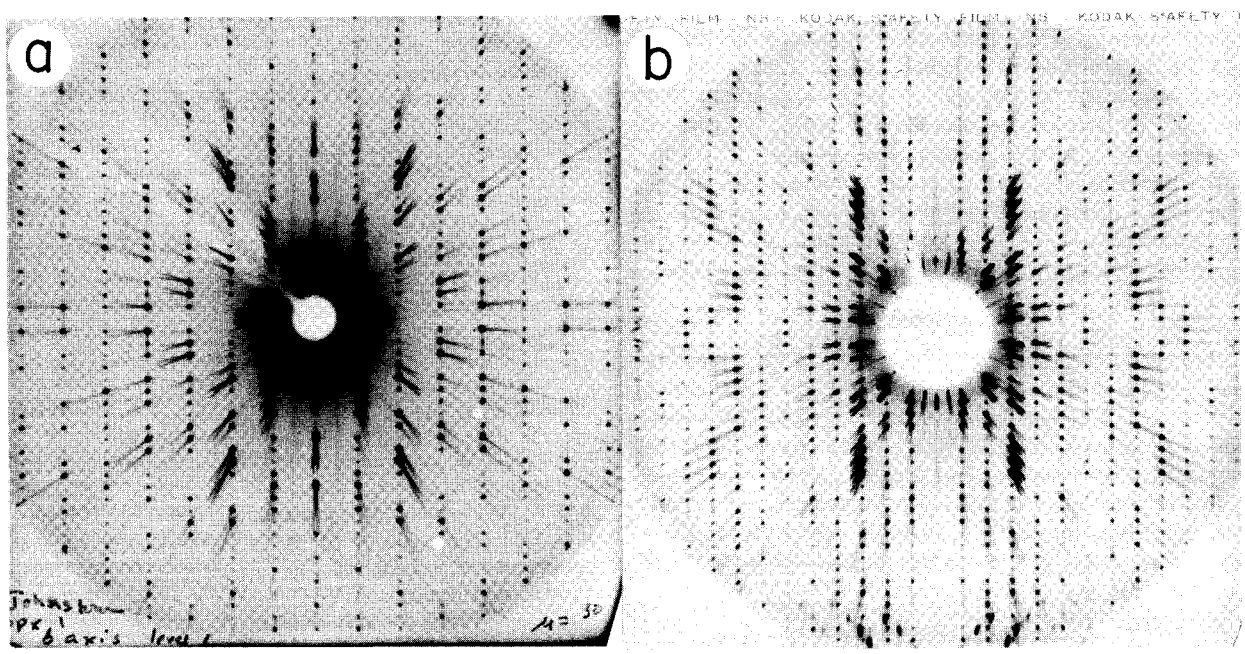

Fig. 6. Long-exposure precession photographs (as in Fig. 5) of (a) ($h1l$) [**a*** trace axis is vertical; 99 hours] and (b) (hkl) [$\mathbf{a}^*_{trace}$ is vertical; 119 hours] layers for enstatite from Johnstown bronzite. Note the continuous streaks through the k = 0 row which cause some of the b-glide plane violations (i.e., $k = 2n + 1$) and the slight increased intensity at k = 0 points as described in the text.

four-circle diffractometer. Therefore these three reflections can be eliminated as supporting a $P2_1ca$ orthopyroxene phase. This leaves only one reflection, 053, which is not adequately explained.

Even though no exsolution was detected optically in lunar pyroxene 78235 (Steele, 1975), the data appear to be consistent with Type I and II diffraction. Considering the Ca content (Wo_3), the annealed provenance (slow cooling or long annealing), and shock history, exsolution and diffuse streaks are expected.

Of the ten orthopyroxene occurrences we studied, two are notable for the number and intensity of "forbidden reflections" and are reported here to compare with the earlier data and to demonstrate the features of more complete data. They are the finely exsolved bronzite from the Johnstown diogenite (AMNH 2495) and a finely exsolved enstatite from southern Zimbabwe (BMNH 1933, 407). Table 1 and Figure 5 show the "forbidden reflections" for these pyroxenes. All of the Type I intensities are consistent with the proposed explanation. Precession photographs of the ($h1l$) and ($hk1$) levels (Fig. 6) demonstrate the effect of diffuse streaks as suggested for Type II "forbidden reflections." All spots are consistent with the expected intensities from Table 2 except 011, 012, and 035, which are slightly too strong for an Opx–Cpx ($C2/c$) intergrowth. This is not considered significant because neither the exact intensities, expected structure factors, nor the diffuseness characteristics were measured or modelled. Moreover, Mori and Takeda (1981) reported the existence of lamellae up to 0.1 μm wide of a $P2_1/c$ clinobronzite phase on (100) of Johnstown pyroxene, which further contributes to the "forbidden reflections" as earlier noted. There does appear to be some concentration of intensity at the locus of "forbidden reflections" that we do not fully understand. However, this feature could be a result of the fine intergrowth structure that leads to diffuseness as well as a possible long-range average structure effect, rather than evidence for a true $P2_1ca$ phase. These two pyroxenes manifest all of the "forbidden reflections" previously used to support a $P2_1ca$ orthopyroxene, and all reflections appear to be amply explained without invoking $P2_1ca$ orthopyroxene.

Conclusions

Almost all reported "forbidden reflections" violating the systematic absences: $k = 2n$ on ($0kl$) of $Pbca$ orthopyroxene can be attributed to one of three diffraction effects described here and, thus, the sytematic absences consistent with a b-glide plane are maintained. Therefore, unless very careful work can prove that legitimate forbidden reflections do, in fact, occur in orthopyroxene diffraction patterns, we must conclude that $P2_1ca$ orthopyroxene is not an established phase.

Acknowledgments

The authors wish to thank Dr. Martin Prinz for supplying the Johnstown pyroxene, Dr. Peter Embrey for the Zimbabwe pyroxene, and Dr. Yoshikazu Ohashi for copies of structure factor data of $P2_1/c$ pyroxenes. This manuscript was improved by the critical reading of Dr. Eric Dowty and Howard Belsky. This work was supported by NSF grant EAR 81-20950 and NASA Grant 7258.

References

Burbank, R. D. (1965) Intrinsic and systematic multiple diffraction. Acta Crystallographica, 19, 957–962.

Evensen, N. M., Hamilton, P. J., Harlow, G. E., Klimentidis, R., O'Nions, R. K. and Prinz, M. (1979) Silicate inclusions in Weekeroo station: planetary differentiates in an iron meteorite. Lunar and Planetary Science, X, 376–377.

Harlow, G. E. (1980) Low orthopyroxene: achondritic abundance and planetary significance. Lunar and Planetary Science, XI, 396–397.

Harlow, G. E., Nehru, C. E., Prinz, M., Taylor, G. J. and Keil, K. (1979) Pyroxenes in Serra de Magé: Cooling history in comparison with Moama and Moore County. Earth and Planetary Science Letters, 43, 173–181.

Huebner, J., Ross, M. and Hickling, N. (1975) Significance of exsolved pyroxenes from lunar breccia 77215. Proceedings Lunar Science Conference 6th, 529–546.

Miyamoto, M., Takeda, H. and Takano, Y. (1975) Crystallographic studies of a bronzite in the Johnstown achondrite. Fortschritte der Mineralogie, Kristallographie und Petrographie, 52, 389–397.

Mori, H. and Takeda, H. (1981) Thermal and deformational histories of diogenites as inferred from their microtextures of orthopyroxene. Earth and Planetary Science Letters, 53, 266–274.

Nord, G. L. Jr. (1980) The composition, structure, and stability of Guinier-Preston zones in lunar and terrestrial orthopyroxene. Physics and Chemistry of Minerals, 6, 109–128.

Nord, G. L., Ross, M. and Huebner, J. S. (1976) Lunar troctolite 76535: mineralogical investigations. Lunar and Planetary Science, VII, 628–630.

Ohashi, Y. and Finger, L. W. (1974) A lunar pigeonite: Crystal structure of primitive-cell domains. Carnegie Institute of Washington Year Book, 73, 525–531.

Papike, J. J., Prewitt, C. T., Sueno, S., and Cameron, M. (1973) Pyroxenes: comparisons of real and ideal structural topologies. Zeitschrift für Kristallographie, 138, 254–273.

Reid, A. M., Williams, R. J. and Takeda, H. (1974) Coexisting bronzite and clinobronzite and the thermal evolution of the Steinbach meteorite. Earth and Planetary Science Letters, 22, 67–74.

Sasaki, S., Fujino, K., Takéuchi Y. and Sadanaga, R. (1980) On the estimation of atomic charges by the x-ray method for some oxides and silicates. Acta Crystallographica, A36, 904–915.

Sasaki, S. and Matsumoto, T. (1977) Multiple diffraction in orthopyroxene: re-examination of the space group. Proceedings of Japan Academy, 53B, 84–89.

Sasaki, S., Matsumoto, T. and Sawada, C. (1981) The influence of multiple diffraction on the space group determination of orthopyroxene, spodumene, low omphacite and pigeonite. Physics and Chemistry of Minerals, 7, 260–267.

Smyth, J. R. (1974) Low orthopyroxene from a lunar deep crustal rock: a new pyroxene polymorph of space group $P2_1ca$. Geophysical Research Letters, 1, 27–29.

Smyth, J. R. (1975) Intracrystalline cation order in a lunar crustal

troctolite. Proceedings Lunar Science Conference 6th, 821–832.

Steele, I. M. (1975) Mineralogy of lunar norite 78235; second lunar occurrence of $P2_1ca$ pyroxene from Apollo 17 soils. American Mineralogist, 60, 1086–1091.

Thompson, J. B. (1970) Geometrical possibilities for amphibole structures: model biopyriboles. American Mineralogist, 55, 292–293.

Manuscript received, October 4, 1982;
accepted for publication, June 27, 1984.